AN INTEGRATED MODEL TO ESTIMATE THE ACCURACY OF DIGITAL ORTHOIMAGES FROM HIGH RESOLUTION SATELLITE IMAGERY

F.J. Aguilar [a, *], M.A. Aguilar [a], F. Carvajal [a], F. Agüera [a]

[a] High Polytechnic School, Department of Agricultural Engineering, Almería University, 04120 La Cañada de San Urbano, Almería, Spain - (faguilar, maguilar, carvajal, faguera)@ual.es

Commission I, WG I/5

KEY WORDS: Earth observation, Very high resolution satellite, Accuracy, Orthorectification, QuickBird, Modelling

ABSTRACT:

In this work, a theoretical-empirical model has been developed for the modelling of the local geometric accuracy of digital orthoimages from panchromatic QuickBird Very High Resolution Satellite Imagery (VHRSI). The empirical component integrates the error of sensor orientation and its propagation to the orthoimage generation process. The theoretical component, mainly a geometrical study from QuickBird Image Metadata File, seeks to model the propagation of DEM error throughout the orthorectificacion process in addition to the previous errors of the bundle adjustment. For the goal of model developing and calibration, a panchromatic QuickBird Basic Imagery was acquired on 19 December 2004, registering a mean collected GSD of 0.62 m, off-nadir view angle of 8.4º and an azimuth and elevation angle of the satellite with respect to the centre of the image of 123.3º and 80.9º respectively. The QuickBird image employed covered an area of 17 x 18 Km over the district of Níjar, located at the North-East of Almería city, Spain. It was centred on the UTM coordinates *European Datum* ED50 (easting and northing) of 577,848 and 4,087,277 m. The Toutin's 3D physical model was the selected method to compute the bundle adjustment and so to carry out the sensor orientation using PCI Geomatica OrthoEngine software v. 9.1.7. On this score, 3D coordinates of 124 ground points were measured by means of high precision differential GPS techniques. From the whole set of ground points, a sub-set of 45 ones uniformly distributed was selected for the sensor orientation (GCPs), whereas the remaining 79 were used as independent check points (ICPs) to assess the performance of the developed model regarding to the average error of the final orthoimages. Inasmuch to the results, the empirical component, which takes into account the effect of pointing error and number and accuracy of GCPs on sensor orientation, presented an acceptable fitting to the experimental data, with a regression coefficient $R^2 = 0.932$. The theoretical component also offered good results, observing like the proposed model reproduces with reasonable accuracy the statistical behaviour of the 2D orthoimage errors measured at the 79 ground points checked. The findings obtained in this work could be used as a guide for the selection of appropriate operational parameters in projects related to digital cartography production and updating from QuickBird imagery.

1. INTRODUCTION

Many researchers have considered the new Very High Resolution Satellite Imagery (VHRSI) as possible substitutes of the classical aerial images used for large scales cartographic purposes (Fraser, 2002; Kay *et al.*, 2003; Chmiel *et al.*, 2004; Pecci *et al.*, 2004; Aguilar *et al.*, 2005), especially in the field of orthoimages production.

Orthoimages are raster maps which store, in a geo-referenced system, a large quantity of graphic information that can be extracted from a particular zone. This type of digital cartography is generated from aerial photographs or satellite images, correcting geometrical deformations caused by the inclination of the optical axis of the central projection and of the relief. For the first correction, it will be necessary a set of ground points which known coordinates both in object space as in image space. For the second correction, it will be necessary an ancillary Digital Elevation Model (DEM).

It is in this field where a very beneficial integration has been taking place in the last few years between the imagery analysis and GIS. Indeed, orthoimages are becoming the main cover of GIS, representing an extraordinary source of thematic information. For instance, the agricultural policies of European Union countries are culminating in the official requirement for the obligatory use of GIS techniques to control the subsidy payments. These Agri-GIS systems require very accurate orthoimages which could be obtained from VHRSI (Rossi and Volpe, 2005).

On the other hand, high resolution orthoimages are contributing to a rapid and cost effective methodology for updating spatial information, which allows for briefer conventional cycles for cartographic updating, highly relevant in GIS orientated to large scales (Baltsavias and Hahn, 1999). It is especially true when VHRSI is used as source image.

But anybody could wonder: which will be the accuracy of the orthorectified product depending on variables such as the number and accuracy of the ground control points (GCPs) employed in the bundle adjustment, Off-nadir view angle, DEM accuracy, image point accuracy, image pointing and so on? (*e.g.* Zhou and Li, 2000; Toutin, 2004a). In more colloquial words, does this cartographic product fit the bill?. Certainly, it would

* Corresponding author. This is useful to know for communication with the appropriate person in cases with more than one author.

be good to know the *a priori* expected accuracy of the final orthoimage and the relative importance of every variable implied, which would help to plan the tasks and resources necessary to ensure the success of the cartographic project and, likely, to save many hours of human work.

In this way, a hybrid (theoretical-empirical) model has been developed for the modelling of the local geometric accuracy of digital orthoimages from panchromatic QuickBird. The empirical component integrates the errors of the bundle adjustment using the rigorous 3D physical model developed at the Canada Centre for Remote Sensing (Toutin, 2004b) and their propagation to the orthoimage generation process. The theoretical component, mainly a geometrical study, seeks to model the propagation of DEM error throughout the orthorectificacion process in addition to the previous errors of the bundle adjustment.

2. STUDY SITE AND DATA SETS

2.1 Study site

The study site comprises an area situated at the North-East of Almería City, Spain, specifically in the region of Campo de Níjar, near to Cabo de Gata's Nature Reserve.

It means a zone occupied principally by greenhouses and with a quite flat relief, excepting the presence of a little range of mountains that crosses the scene along direction South-West (so-called Serrata) and the mountain range of Sierra Alhamilla, located at the North-West of the scene. The working area used for this paper presents an approximated elevation range of between 45 m to 850 m above mean sea level.

2.2 QUICKBIRD Basic Imagery and Ground Control Points

For the goal of model development and calibration, a panchromatic QuickBird Basic Imagery was acquired on 19 December 2004, registering a mean collected GSD of 0.62 m, radiometric resolution of 11 bits, off-nadir view angle of 8.4º and an azimuth and elevation angle of the satellite with respect to the centre of the image of 123.3º and 80.9º respectively. The QuickBird image employed covered an area of 17 x 18 Km over the district of Níjar (Fig. 2) and was centred on the geographic coordinates WGS84 of N 36.93045º and W 2.12685º.

The 3D Toutin physical model (Toutin and Cheng, 2002; Toutin, 2003), based in the widely known collinearity equation in the CCD-line direction, was the selected method to compute the bundle adjustment and so to carry out the sensor orientation using PCI Geomatica OrthoEngine software v. 9.1.7.

On this score, 3D coordinates of 124 ground points were measured by means of high precision differential GPS techniques (Fig. 2), presenting an average accuracy, expressed as Root Mean Square Error (RMSE) as follows: $RMSE_x$ = $RMSE_y$ = 10 cm and $RMSE_z$ = 15 cm. From the whole set of ground points, a sub-set of 45 ones uniformly distributed was selected for the sensor orientation (GCPs). This uniform distribution was achieved dividing the whole scene into 3 by 3 sub-areas (see the grid on the Fig. 1) and collecting the GCPs used in every case as a multiple of 9, *i.e.*, an equal sized number of GCPs belonging to each one of the sub-areas. The remaining 79 ground points were used as independent check points (ICPs) to assess the performance of the developed model regarding to the average error of the final orthoimages. The ICPs presented a range of between 68 m to 247 m, with a mean value of 171 m.

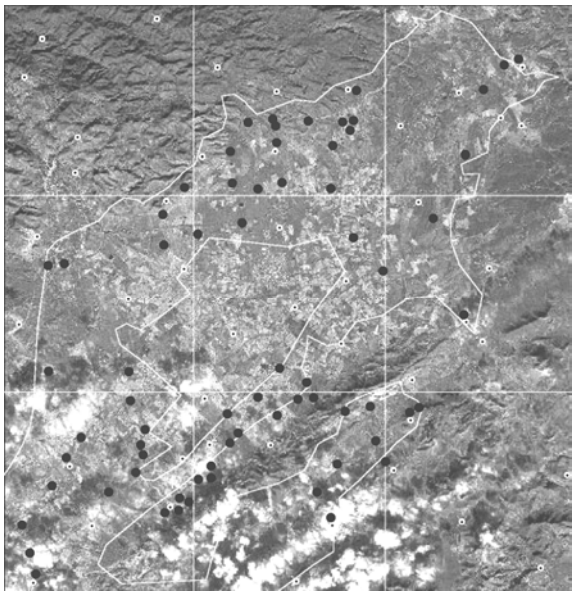

Figure 1. Distribution of ICPs (black circles) and GCPs (black points inside white circles) overlaid on the QuickBird Basic Imagery. © QuickBird Image Copyright 2004, DigitalGlobe®.

2.3 Digital Elevation Models

For the production of panchromatic orthoimages from QuickBird, three grid DEMs were employed as ancillary data for checking the performance of the developed model:

a) A coarse 20 m grid spacing DEM produced by the Environmental Council of the Andalusia Government, extracted from the 1:50,000 National Topographic Map series (contour interval of 20 m). It presented a vertical RMSE, measured over 50 DGPS check points, of about 5.8 m.

b) A medium accuracy DEM, 5 m grid spacing, derived by ourselves from digitized contour lines extracted from the 1:10,000 Andalusia Topographic Map series (contour interval of 10 m). It presented a vertical RMSE, measured over 50 DGPS check points, of about 1.75 m.

c) A dense DEM, 2 m grid spacing, generated by ourselves from a 1:5,000 scale photogrammetric aerial flight. This DEM was carried out by means of stereo-matching techniques over digital images and afterward revised and edited by an operator (Karras *et al.,* 1998). It presented a vertical RMSE, measured over 50 DGPS check points, of about 0.31 m.

2.4 Orthoimages production

Digital orthoimages were created presenting a GSD of 0.6 m. As is fully known, the orthorectification process comprises a digital resampling procedure that can influence on the accuracy of the final results. So we applied for every orthoimage the same resampling kernel, in this case the sinusoidal one (sin(x)/x

over a 16x16 pixels window), recommended by some authors as the most accurate (Toutin, 2004a).

3. MODEL DEVELOPMENT

The full model developed in this work can be expressed as a sum of two components:

$$\sigma^2_{ortho} = \sigma^2_{BA} + \sigma^2_{DEM} \quad (1)$$

Where σ^2_{ortho} is the final two-dimensional error of the orthoimage, σ^2_{BA} is the bundle adjustment error or sensor orientation error, and σ^2_{DEM} is the 2D orthoimage error propagated from the original DEM error. All the terms are expressed as error variances.

Equation 1 is based on the general error-propagation theory, assuming that the sources of error are independent or uncorrelated and, likewise, that the errors are randomly distributed. Notice that equation 1 can be expressed in terms of RMSE because RMSE is close to the value of standard deviation (σ) when the mean error tends to be zero (unbiased residuals). Really, this approach could be considered as an important shortcoming about the practical application of the model. In fact, errors at check points do not use to be exclusively random under operational conditions, but they can usually show a non negligible systematic component, especially when check points have been digitized from a map. In these cases a careful removal of systematic errors should be afforded before applying the proposed model.

3.1 Empirical component regarding to the bundle adjustment error

The calibration parameters of the empirical component of the proposed model (Eq. 2), *i.e.*, the term σ^2_{BA} in equation 1, were obtained by nonlinear regression. A sigmoidal model skeleton, previously detected from the graphical shape of plotted data (see figure 4), was selected as the best model describing the behaviour of experimental data. The Marquardt iterative search algorithm was used to determine the estimates that minimize the residual sum of squares. The sources of variation taken into account were those reported by some authors as the most relevant (Tao and Hu, 2002; Toutin and Cheng, 2002; Tao *et al.*, 2004), *i.e.* number, location and accuracy of the GCPs. Furthermore, it was introduced the error of image pointing, because it can become the predominant error when GCPs present a high accuracy (Toutin and Chénier, 2004), for example in the case of DGPS collection.

$$\sigma_{BA} \approx \mathrm{RMSE}_{\mathrm{BA}} = \frac{(1+105.805.N^{-1.0879}).RMSE_{plotting}.e^{0.0447.SDA}}{1+105.805.N^{-1.0879}.e^{-0.4849.SDA}} \quad (2)$$

Being N the number of GCPs used for the bundle adjustment, SDA the sample data accuracy or GCPs accuracy and $\mathrm{RMSE}_{\mathrm{plotting}}$ the image point accuracy or plotting error measured as root mean square error at the ground space.

Because by the lack of variation of the GCPs accuracy, original GCPs error was perturbed to raise the range of variation of the variable GCPs accuracy, since it could notably improve the statistical robustness of the empirical model adjustment by nonlinear regression. It was carried out using statistical simulation, *i.e.* by the addition of a value to the original coordinates X, Y, Z of every GCP. The aforementioned value was extracted from a population with a normal distribution of zero mean and standard deviation corresponding to the perturbed GCPs wished error. That is to say, a normal and controlled error was added to original GCPs to obtain a wide range of GCPs 3D accuracy, from 0.2 m (the high original accuracy) to 34.6 m (obviously a quite poor accuracy). The number of GCPs employed in the bundle adjustment, considered as another variable else, was ranged as a multiple of the 9 sub-areas in which the working area was previously divided (Fig. 2), resulting the following values: 9, 18, 27, 36 and 45 GCPs. Furthermore a stratified random sampling (9x9 sub-areas) was used to acquire four replicates for every number of GCPs tested.

3.2 Theoretical component regarding to DEM to orthoimage error

The second component of the full model, the planimetric point displacement due to the propagation of the DEM error through the orthorectification process, was estimated exclusively by geometrical considerations from the QuickBird Image Metadata File, deducing the equation 3 for a generic point P. The algebra from which equation 3 is derived is rather tedious and purely geometrical, and so has not been included in this paper. However, figures 2 and 3 lay out some of the geometrical considerations taken into account for the development of equation 3. For example it is important to note the influence of slope and aspect for each point because pixel displacement can be increased or decreased depending on the orientation of terrain regarding to satellite sight (see details A and B in figure 2).

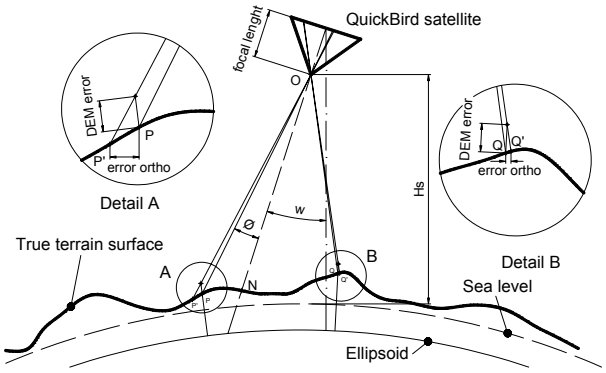

Figure 2. Transversal view of the image acquisition geometry.

In equation 3, tanα is the local terrain slope at point P, whereas the angle τ (degrees) is the local terrain aspect at the same point, both of them computed from a 2 m grid spacing DEM. In this way, the aspect at each grid node was calculated as angle which exists between direction north and the projection on the horizontal plane of the slope vector normal to the DEM surface (0º points to the north and 90º points to the east).

$$\sigma_{DEM} \approx \mathrm{RMSE}_{\mathrm{DEM}} = \frac{\Delta S_P \left[\sqrt{1-\left(\frac{\Delta S_P}{R_{earth}}\right)^2} + \frac{Hs}{R_{earth}} \right].RMSE_z}{Hs-[A+B]} \quad (3)$$

$$A = \tan\alpha.\sin\tau.(Hs.\tan\omega.\sin\gamma + x_P - x_N) \quad (4)$$

$$B = \tan\alpha.\cos\tau.(Hs.\tan\omega.\cos\gamma + y_P - y_N) \quad (5)$$

Following with equation 3, $RMSE_z$ (m) represents the DEM accuracy at point P, which can obviously vary from a point to other, although, in this work, will be used an average value for the whole of the working area. Off-nadir view angle (degrees) comes given by w, and R_{earth} is the earth radius (m). X_N and Y_N are the UTM coordinates (m) of the image centre, *i.e.* the theoretical nadir if w = 0, whereas X_P and Y_P are the corresponding UTM coordinates (m) of the point P. H_s would be the approximate orbit altitude (450,000 m), γ the target azimuth (303.3º in our case, see figure 3) and, finally, ΔS_P is the distance between point P and the real nadir according to the current off-nadir view angle of the scene. Figure 3 shows an aerial view of the image registration, highlighting the large ground distance between the scene center and the real nadir (satellite perpendicular projection regarding to the earth surface).

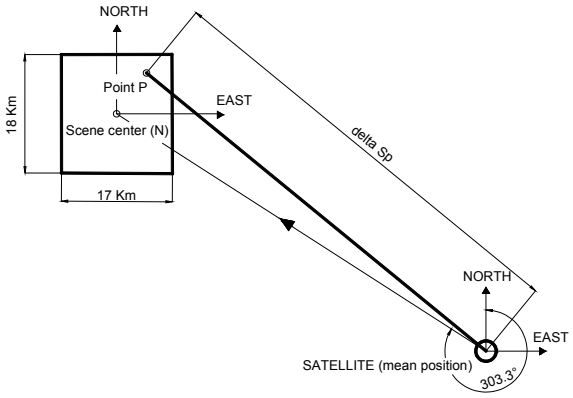

Figure 3. Aerial view of the image acquisition geometry.

4. RESULTS AND DISCUSSION

4.1 Empirical component adjustment

The empirical model presented at equation 2 showed an acceptable fitting to the experimental data, with a R^2 regression coefficient of 0.932 (Fig. 3). Notice that $RMSE_{plotting}$ (Eq. 2) can usually take values between 0.5 and 2 pixels (Li *et al.,* 2002). For the presented adjustment, an average value of 1 pixel (approximately 0.62 m ground pixel size) was taken. It must also be highlighted that RMSE along vertical axis in figure 4 was computed over the 79 ICPs which were not utilized for the bundle adjustment.

It is important to notice about the sigmoidal nature of the model showed in figure 4. It implies certain continuity about sensor orientation error on medium ranges GCPs accuracy levels, above all working with a reasonably large number of GCPs. As we can also see in figure 3, the effect of number of GCPs is much stressed, mainly when GCPs accuracy tends to get down. Shortly, the more accurate GCPs we have the less number of them we need.

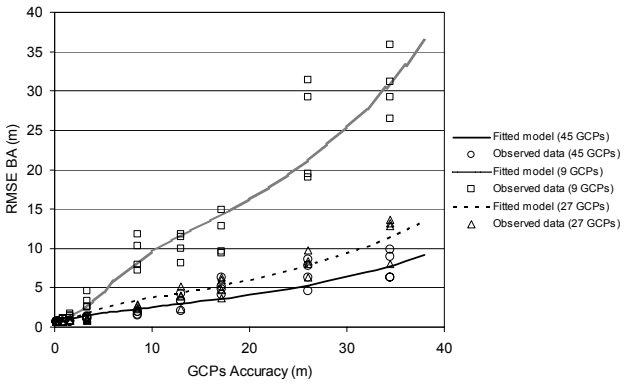

Figure 4. Bundle adjustment error according to the different number and accuracy of GCPs used for sensor orientation.

4.2 Validation of the developed model

The full model described on the last sections was validated over the ground planimetric coordinates of 79 ICPs measured manually at the orthoimages, testing the effect produced by the use of the three DEMs referred at the section 2.3.

The results that appear in table 1 are based on the hypothesis of normal distribution of the orthoimage residuals over the whole of the scene. Thus, supposing the error at every point i as a random variable of zero mean and standard deviation σ_{orthoi} given by equation 1, it is possible to compute an average standard deviation (σ_{ortho}) for the whole working area and, therefore, to use this parameter for calculating different probability areas from a normal distribution. For example, around 68% of observed residuals should be comprised within the bounds ± σ_{ortho}, whereas 99.7% should be within ±3 σ_{ortho} bounds. According to this, the results showed in table 1 can be considered as reasonably close to expected or theoretical values, excepting the interval of amplitude σ where the developed model always underestimate the target value of 68%. It must be pointed out that we have only a finite number of ICPs and, so, whatever estimation is merely an approximation to the real distribution of residuals.

As an additional measure about the performance of the developed model, orthoimage RMSE over the 79 available ICPs was calculated (observed RMSE) and later compared with RMSE estimated by the model, considering orthoimage residuals as fully independent random variables. From results showed in table 2, it can be reported a good agreement between estimated and observed RMSEs for each one of the DEMs tested in this work, although, for all cases, the model underestimated the observed values. Since GCPs accuracy used for sensor orientation is the highest one ($RMSE_{GCPs}$ = 0.2 m), differences due to an increase on the number of GCPs are practically negligible within the same DEM. Equally, the error predicted by the model is little sensible to DEM accuracy when this is sufficiently low. The last tendency is also noticed on observed RMSEs.

Regarding to the behavior of maximum errors, table 2 shows a similar tendency between observed and estimated values, although they present larger differences than in the last case of

RMSE comparison, above all working with the low accuracy DEM. Notice that estimated value was calculated following 3σ rule and, furthermore, observed maximum error was obtained from a relatively small sample of 79 ICPs.

DEM accuracy and GCPs used in sensor orientation	Estimated probability area (%)			
	σ	1.64σ	1.96σ	3σ
$RMSE_z$ = 5.8 m (9 GCPs)	54.43	83.54	94.93	100
$RMSE_z$ = 5.8 m (45 GCPs)	50.63	89.87	98.73	100
$RMSE_z$ = 1.75 m (9 GCPs)	62.02	92.40	93.67	100
$RMSE_z$ = 1.75 m (45 GCPs)	51.89	89.87	94.93	100
$RMSE_z$ = 0.31 m (9 GCPs)	60.75	89.87	96.20	98.73
$RMSE_z$ = 0.31 m (45 GCPs)	60.75	89.87	94.93	98.73
Theoretical value	68	90	95	99.7

Table 1. Probability area regarding to statistical distribution of residuals. Results for the highest GCPs accuracy ($RMSE_{GCPs}$ = 0.2 m)

DEM accuracy and GCPs used in sensor orientation	Errors (m)			
	E_{est}	E_{obs}	ME_{est}	ME_{obs}
$RMSE_z$ = 5.8 m (9 GCPs)	1.14	1.29	3.64	2.59
$RMSE_z$ = 5.8 m (45 GCPs)	1.13	1.23	3.61	2.36
$RMSE_z$ = 1.75 m (9 GCPs)	0.73	0.78	2.24	1.83
$RMSE_z$ = 1.75 m (45 GCPs)	0.72	0.82	2.19	1.91
$RMSE_z$ = 0.31 m (9 GCPs)	0.68	0.74	2.05	2.16
$RMSE_z$ = 0.31 m (45 GCPs)	0.66	0.75	1.99	2.16

Table 2. Comparison between estimated and observed orthoimage error. E_{est} = estimated RMSE; E_{obs} = observed RMSE; ME_{est} = estimated maximum error ($3RMSE_{est}$); ME_{obs} = observed maximum error. Results for the highest GCPs accuracy ($RMSE_{GCPs}$ = 0.2 m)

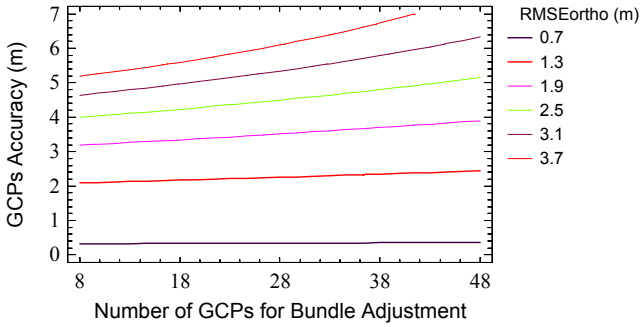

Figure 5. Effect of number and accuracy of GCPs on orthoimage accuracy.

According to the proposed model, orthoimage accuracy *versus* number and accuracy of GCPs is depicted in figure 5. From this figure we can estate that number of GCPs is practically irrelevant for orthoimage accuracy working with high accuracy GCPs (RMSE below 2-3 m would be enough). Let us remember that Toutin's sensor orientation model requires a theoretical minimum of six GCPs for Basic Imagery. However, it is necessary to use a larger number of GCPs when GCPs accuracy tends to make worse (RMSE around 4 m or more).

Since errors are unavoidable when measuring ground points from images (image coordinates), even if they are clearly well-defined, it would be interesting to assess the impact of this type of error (so-called pointing or plotting error) on orthoimage accuracy. It is showed in figure 6. The results obtained from the proposed model demonstrate that pointing error always represents an important source of error, but this effect is more pronounced when GCPs accuracy is excessively low (RMSE around 1 m or more). Let us think about normal range of variation of pointing error on VHRSI uses to be in the order of 0.5 to 2 pixels (0.3 to 1.2 m for QuickBird imagery). So it should be limited by means of selecting ground points defined as well as possible on digital image.

Finally, figure 7 allows recommending the use of accurate DEMs when off-nadir view angle is very pronounced. Indeed for accurate orthoimage production, an off-nadir view angle below 10º should be considered working from non accurate DEMs.

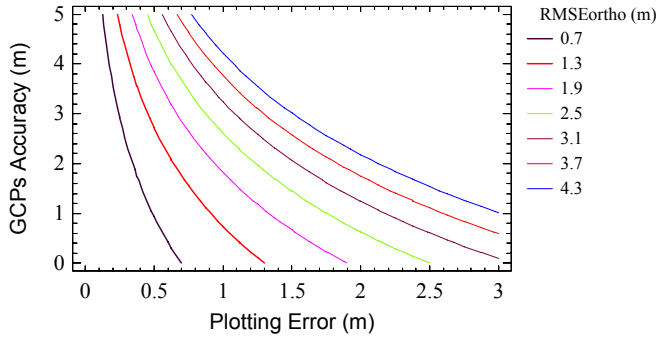

Figure 6. Effect of GCPs accuracy and pointing error on orthoimage accuracy.

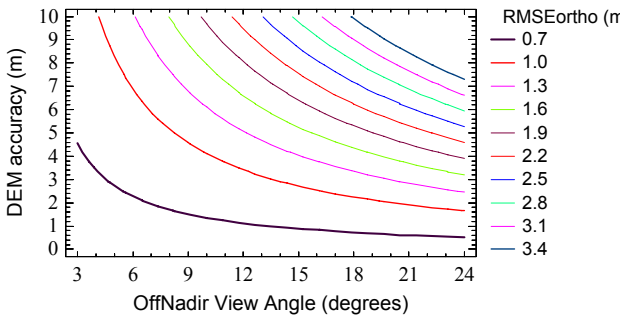

Figure 7. Effect of vertical DEM accuracy and Off-nadir view angle on orthoimage accuracy.

5. CONCLUSIONS

We have developed a hybrid model which allows the modeling of the local geometric accuracy of digital orthoimages from panchromatic QuickBird VHRSI.

The empirical component, which takes into account the effect of pointing error and number and accuracy of GCPS on sensor orientation by means of Toutin's 3D physical model, presented an acceptable fitting to the experimental data, with a regression coefficient $R^2 = 0.932$.

The theoretical component, related to the local planimetric point displacement due to the propagation of the DEM error through the orthorectification process, was estimated exclusively by geometrical considerations from the QuickBird Image Metadata File. The results have resulted to be very promising, observing like the proposed model reproduces with reasonable accuracy the statistical behavior of the 2D orthoimage errors measured at the 79 ground points checked.

The findings obtained in this work could be used as a guide for the selection of appropriate operational parameters in projects related to digital cartography production and updating from QuickBird imagery.

Finally, and as a shortcoming, it should be beard in mind that the model has not taken into account GCPs distribution. Indeed, GCPs distributed on a straight line across the track (Li *et al.,* 2002) or not covering the whole of the scene both in horizontal projection as along vertical direction (Toutin, 2003) constitute a weak geometric configuration and it should be further on introduced in the model.

6. ACKNOWLEDGEMENTS

The authors would like to thank Public Company for Agriculture and Fishery of Andalusia (D.a.p.) for its collaboration. This research work has been carried out within the project "Generation, integration and updating of digital cartography as a support for rural sustainable development. Methodology and application in Campo de Níjar (Almería)". It has been founded by Andalusia Government.

7. REFERENCES

Aguilar, M.A., Aguilar, F.J., Sánchez, J.A., Carvajal, F. and Agüera, F., 2005. Geometric correction of the QuickBird high resolution panchromatic images. In: *XXII International Cartographic Conference*, A Coruña, Spain. Unpaginated CD ROM.

Baltsavias, E.P., and Hahn, M., 1999. Integration of image analysis and GIS. *International Archives of Photogrammetry and Remote Sensing*, 32(part 7-4-3W6), pp. 12-19.

Chmiel, J., Kay, S. and Spruyt, P., 2004. Orthorectification and geometric quality assessment of very high spatial resolution satellite imagery for Common Agricultural Policy purposes. *The International Archives of the Photogrammetry, Remote Sensing and Spatial Information Sciences*, Istambul, Turkey, Vol. XXXV, Part B4, 5 p. (On DVD).

Fraser, C.S., 2002. Papers of ACRS 2002 "Prospect for mapping from high-resolution satellite imagery", Kathmandu, Nepal. www.gisdevelopment.net/aars/acrs/2002/vhr/070.pdf (last accessed 2 May 2006).

Karras, G.E., Mavrogenneas, N., Mavrommati, D. and Tsikonis, N., 1998. Tests on automatic DEM generation in a digital photogrammetric workstations. *International Archives of Photogrammetry and Remote Sensing,* 32(2), pp. 136-139.

Kay, S., Spruyt, P., Alexandrou, K., 2003. Geometric quality assessment of orthorectified VHR space image data. *Photogramm. Eng. Remote Sens*., 69(5), pp. 484-491.

Li, R., Zhou, G., Schmidt, N.J., Fowler, C. and Tuell, G., 2002. Photogrammetric processing of high-resolution airborne and satellite linear array stereo images for mapping applications. *International Journal of Remote Sensing*, 23(20), pp. 4451-4473.

Pecci, J., Cano, F. and Maza, G., 2004. Generación de una ortoimagen QuickBird del año 2003 de la Comunidad Autónoma de la Región de Murcia: metodología y resultados. In: *XI Congreso Métodos Cuantitativos, Sistemas de Información Geográfica y Teledetección*, Murcia, Spain. Vol. I, pp. 301-312.

Rossi, L. and Volpe, F., 2005. Integrated cadastre system for EU agricultural subsidies. Italian response to the challenge of environmental sustainability. *GEOinformatics*, 8(4), pp. 12-13.

Tao, C.V. and Hu, Y., 2002. 3-D reconstruction methods based on the rational function model. *Photogrammetric Engineering and Remote Sensing*, 68(7), pp. 705-714.

Tao, C.V., Hu, Y. and Jiang, W., 2004. Photogrammetric exploitation of IKONOS imagery for mapping applications. *International Journal of Remote Sensing*, 25(14), pp. 2833-2853.

Toutin, T. and Cheng, P., 2002. QuickBird- A milestone for high-resolution mapping. *Earth Observation Magazine*, 11(4), pp. 14-18.

Toutin, T., 2003. Error tracking in Ikonos geometric processing using a 3D parametric model. *Photogrammetric.Engineering and Remote Sensing.*, 69(1), pp. 43-51.

Toutin, T., 2004a. Review article: Geometric processing of remote sensing images: models, algorithms and methods. *International Journal of Remote Sensing*, 25(10), pp. 1893-1924.

Toutin, T., 2004b. Comparison of stereo-extracted DTM from different high-resolution sensors: SPOT-5, EROS-A, IKONOS-II, and QuickBird. *IEEE Transactions on Geoscience and Remote Sensing*, 42(10), pp. 2121-2129.

Toutin, T. and Chérnier, R., 2004. GCP requirement for high-resolution satellite mapping. *International Archives of Photogrammetry, Remote Sensing and Spatial Information Sciences*. Istambul, Turkey, Vol. XXXV, Part B3, 6 p. (On DVD).

Zhou, G. and Li, R., 2000. Accuracy evaluation of ground points from IKONOS high-resolution satellite imagery. *Photogrammetric Engineering and Remote Sensing*, 66(9), pp.1103-1112.